Frustrated minority spins in GeNi$_2$O$_4$

Frustrated minority spins in GeNi$_2$O$_4$

M. Matsuda[1], J.-H. Chung[2], S. Park[3], T. J. Sato[4], K. Matsuno[5], H. Aruga Katori[6,7], H. Takagi[5,6,7],
K. Kakurai[1], K. Kamazawa[8], Y. Tsunoda[9], I. Kagomiya[9], C. L. Henley[10] and S.-H. Lee[8(a)]

[1] *Quantum Beam Science Directorate, Japan Atomic Energy Agency - Tokai, Ibaraki 319-1195, Japan*
[2] *Department of Physics, Korea University - Seoul, Korea*
[3] *HANARO Center, Korea Atomic Energy Research Institute - Daejeon, Korea*
[4] *The Institute for Solid State Physics, University of Tokyo - Kashiwa, Chiba 277-8581, Japan*
[5] *Graduate School of Frontier Sciences, University of Tokyo - Kashiwa, Chiba 277-8561, Japan*
[6] *RIKEN (The Institute of Physical and Chemical Research) - Wako, Saitama 351-0198, Japan*
[7] *CREST, Japan Science and Technology Corporation - Saitama 332-0012, Japan*
[8] *Department of Physics, University of Virginia - Charlottesville, VA 22904, USA*
[9] *Department of Applied Physics, Waseda University - 3-4-1 Okubo, Shinjuku-ku, Tokyo 169-8555, Japan*
[10] *Department of Physics, Cornell University - Ithaca, NY 14853-2501, USA*

Abstract – Recently, two consecutive phase transitions were observed, upon cooling, in an antiferromagnetic spinel GeNi$_2$O$_4$ at $T_{N1} = 12.1$ K and $T_{N2} = 11.4$ K, respectively (Crawford M. K. *et al.*, *Phys. Rev. B*, **68** (2003) 220408(R)). Using unpolarized and polarized elastic neutron scattering we show that the two transitions are due to the existence of frustrated minority spins in this compound. Upon cooling, at T_{N1} the spins on the $\langle 111 \rangle$ kagome planes order ferromagnetically in the plane and antiferromagnetically between the planes (phase I), leaving the spins on the $\langle 111 \rangle$ triangular planes that separate the kagome planes frustrated and disordered. At the lower T_{N2}, the triangular spins also order in the $\langle 111 \rangle$ plane (phase II). We also present a scenario involving exchange interactions that qualitatively explains the origin of the two purely magnetic phase transitions.

In spinels AB$_2$O$_4$, the B sites form a highly frustrating network of corner-sharing tetrahedra, sometimes called a pyrochlore lattice [1,2]. In the limit of only nearest-neighbor antiferromagnetic, isotropic exchange interactions, this system has macroscopic ground-state degeneracy, leading to a spin liquid state down to zero temperature [3–5], or to ordering at unobservably low temperature [6]. The ground-state degeneracy can however be lifted when the spin is coupled with lattice or orbital degrees of freedom. For instance, a spin-lattice coupling can induce a phase transition where a magnetic ordering and a lattice distortion occur simultaneously [7–9]. When an orbital degeneracy is present, a Jahn-Teller distortion usually occurs first upon cooling to lift the orbital degeneracy. If the resulting magnetic interactions are

three dimensional, then a magnetic ordering occurs simultaneously. On the other hand, if the effective magnetic interactions in the distorted phase become low dimensional, the magnetic ordering is suppressed and may occur at a lower temperature, yielding two successive phase transitions [10–12]. Thus, it was surprising when GeNi$_2$O$_4$ exhibited two successive phase transitions in spite of the absence of an orbital degeneracy of Ni^{2+} ($3d^8$) ions [13]. No structural distortion was observed by synchrotron X-ray or by neutron scattering measurements, indicating that the transitions are purely magnetic [13].

When viewed along the $\langle 111 \rangle$ direction, the pyrochlore lattice can be described as alternating layers of a kagome (of corner-sharing triangles) and a triangular lattice (with 1/3 as many spins per layer as the kagome layer). We have performed polarized and unpolarized elastic neutron scattering measurements on a single crystal of GeNi$_2$O$_4$

(a)E-mail: shlee@virginia.edu

to understand the nature of the phase transitions. Our results show that upon cooling, at T_{N1} the kagome (majority) spins order ferromagnetically in the $\langle 111 \rangle$ plane and antiferromagnetically between the planes (phase I). Our polarized elastic neutron scattering indicates that the kagome spins are aligned along a high-symmetry direction in the kagome plane. The antiferromagnetic stacking of the kagome planes induces zero internal magnetic field at the triangular spins that lie between the kagome planes and leaves the triangular spins frustrated. The triangular spins order in the $\langle 111 \rangle$ plane only at the lower $T_{N2} = 11.4$ K. In order to understand the experimental findings, we have considered a spin Hamiltonian with superexchange interactions among Ni^{2+} ions up to the fourth nearest neighbors. The model shows that dominant ferromagnetic J_1 and antiferromagnetic J_4 are the key interactions driving the first phase transition at T_{N1}, which is consistent with the Goodenough-Kanamori rules. However, it calls for ferromagnetic J_3 and antiferromagnetic J_3' to describe the triangular-layer behavior, which does not seem to obey the rules.

A single crystal of $GeNi_2O_4$ was grown by the chemical vapor transport method using $TeCl_4$ as a transport agent. The crystal has the shape of an octahedron, an edge of which is typically about 1 mm long. Details of the sample characterization are described elsewhere. The elastic neutron scattering experiments using unpolarized neutrons were carried out on the thermal neutron triple-axis spectrometer TAS2 installed at the guide hall of JRR-3 at Japan Atomic Energy Agency. The energy of scattered neutrons was fixed to be 14.7 meV. The horizontal collimator sequences were guide-80′-S-80′-80′ or guide-80′-S-80′-open. Polarized neutron scattering experiments were carried out on the thermal neutron triple-axis spectrometers TAS-1 installed at the beam hall of JRR-3. Heusler alloy (111) fixed to 14.7 meV was used as monochromator and analyzer. A flipping ratio of ~ 25 was obtained on some nuclear Bragg peaks. The single crystal was mounted with the [111] and [01$\bar{1}$] axes in the horizontal scattering plane, while a vertical guide field was applied. Contamination from higher-order beams was effectively eliminated using PG filters.

Bertaut *et al.* have performed neutron diffraction measurements [14] on a powder sample of $GeNi_2O_4$ and showed that at 4 K spins are in a long-range ordered state with a characteristic wave vector $\boldsymbol{Q} = (1/2, 1/2, 1/2)$. They have proposed as the ground state a collinear spin structure in which, as shown in fig. 2(a), the spins in kagome and triangular planes are aligned ferromagnetically in each plane and are stacked antiferromagnetically along the (111) direction. Our unpolarized elastic neutron scattering on a single crystal of $GeNi_2O_4$ confirmed the characteristic wave vector being $\boldsymbol{Q} = (1/2, 1/2, 1/2)$. Figure 1(a) shows the temperature dependence of the magnetic Bragg intensities at $\boldsymbol{Q} = (\frac{1}{2} \frac{1}{2} \frac{1}{2})$ and $(\frac{1}{2} \frac{1}{2} \frac{\bar{3}}{2})$, obtained from the single crystal of $GeNi_2O_4$. Both data
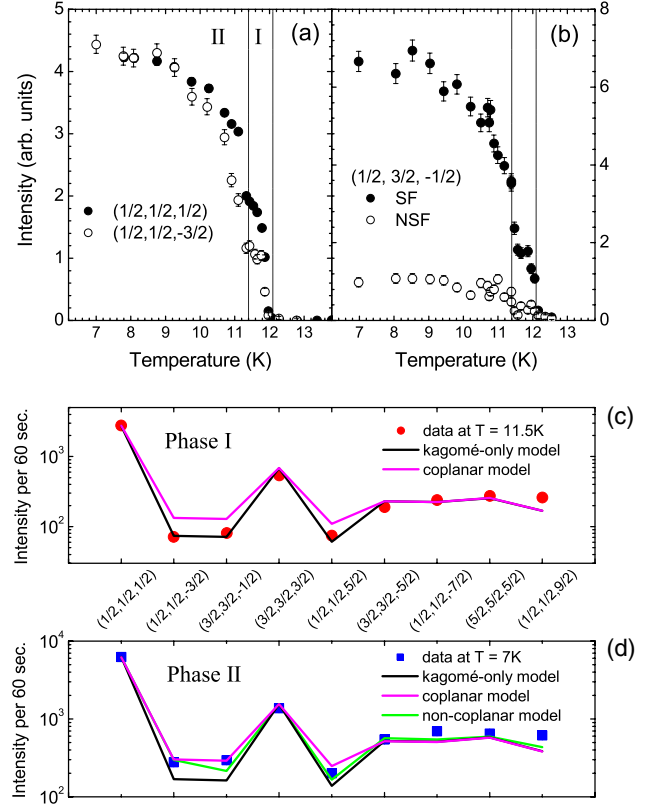

Fig. 1: (Colour on-line) Temperature dependence of the peak intensity of the $(\frac{1}{2}, \frac{1}{2}, \frac{1}{2})$ and $(\frac{1}{2}, \frac{1}{2}, \frac{3}{2})$ magnetic Bragg reflections measured with unpolarized neutrons (a), and that of the $(\frac{1}{2}, \frac{1}{2}, \frac{\bar{3}}{2})$ magnetic Bragg reflections measured with polarized neutrons (b). The vertical lines correspond to the two transition temperatures. Experimental and calculated integrated intensities for magnetic reflections using unpolarized neutrons at $T = 11.5$ K (c) and 7 K (d).

show a sharp increase in intensity around 12.1 K (phase I) with another sharp increase around 11.4 K (phase II), which indicates the existence of two distinct magnetic transitions and is consistent with the recent neutron powder diffraction data [13].

Our single-crystal data, however, allow us to study the nature of the phase transitions in more detail than the previous powder diffraction studies. The ratio of the intensities of the two reflections, $I(\frac{1}{2}, \frac{1}{2}, \frac{1}{2})/I(\frac{1}{2}, \frac{1}{2}, \frac{3}{2})$, changes as the system goes from phase I to phase II. This indicates that phases I and II have different spin structures. In order to investigate the ordered states in detail, we have performed unpolarized elastic scattering at nine independent magnetic Bragg reflections at 7 K (phase II) and 11.5 K (phase I). The scans were made along the longitudinal directions in the momentum space. Their integrated intensities are summarized in a log scale in figs. 1(c) and (d). The data were fitted to spin structures that are allowed by a linear combination of the basis vectors of irreducible representations for the $Fd\bar{3}m$ group with $\boldsymbol{Q} = (\frac{1}{2} \frac{1}{2} \frac{1}{2})$ [15,16]. Since there is a 3-fold symmetry
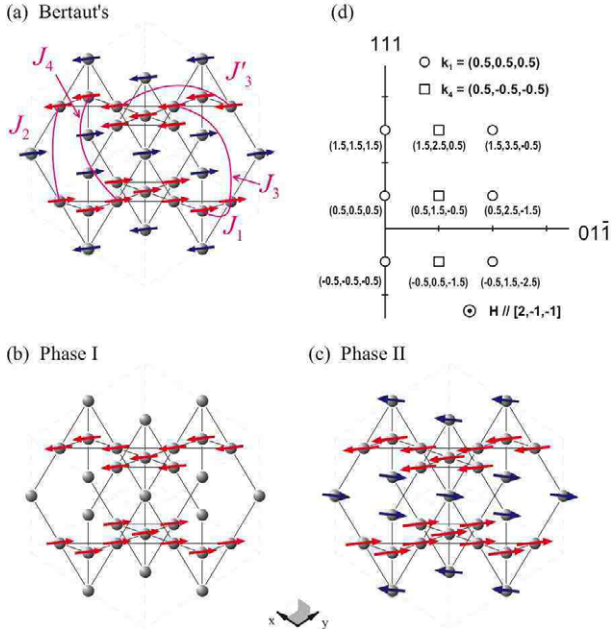
Fig. 2: (a) Bertaut's collinear spin model. (b) A collinear spin model for phase I with only kagome spins ordered. (c) A non-collinear spin model for phase II. All the spins are lying within the (111) plane, while the triangular and the kagome spins are pointing $\sim 60°$ away from each other. (d) The diagram of the horizontal scattering plane for the polarized neutron measurements. The circles and squares represent the magnetic Bragg reflections from the k_1 and k_4 domains, respectively. The guide field was applied perpendicular to the plane along $[2\bar{1}\bar{1}]$.

within either triangular or kagome planes, the calculated intensities were averaged among three equivalent spin orientations.

Interestingly, the collinear spin structure proposed by Bertaut *et al.* (fig. 2(a)) [14] could not reproduce our phase-I data. Furthermore, none of the coplanar models where all spins lie on the same plane could fit our data, as long as both kagome and triangular spins are ordered[1] (see the pink on-line line in fig. 1(c)). Instead, the data was best fitted to a spin structure with only the kagome spins ordered with $\langle M \rangle^{\mathrm{I}}_{\mathrm{kag}} = 1.3 \mu_{\mathrm{B}}$ and with the triangular spins disordered (the black on-line line in fig. 1(c)). This ordering of partial spins can be understood when we consider the internal magnetic field at the triangular sites due to the neighboring kagome spins. Since the triangular plane is sandwiched by two kagome planes below and above, the internal magnetic fields due to the two kagome planes cancel each other on the triangular sites. Thus, even when the system cools down and the kagome spins order, the triangular spins lying in between the kagome planes cannot order.

---

[1]Note that the observed intensities averaged among three S-domains are independent of the spin orientations within kagome planes.

When the system cools further down to phase II, the relative intensities of the magnetic Bragg reflections change (fig. 1(d)), indicating that the spin structure is different from that of phase I. Since the unpolarized neutron scattering data are rather insensitive to the orientation of the weak triangular spins, the data can be reproduced equally well by several models: any coplanar models (see figs. 2(a) or (c)) with both the triangular and the kagome spins ordered within the (111) plane with $\langle M \rangle^{\mathrm{II}}_{\mathrm{kag}} = \langle M \rangle^{\mathrm{II}}_{\mathrm{tri}} = 1.8 \mu_{\mathrm{B}}$ (purple on-line line in fig. 1(d)), to which the Bertaut's model belongs, and non-coplanar models where the triangular spins are aligned perpendicular to the (111) plane whereas the kagome spins are in the plane. In the non-coplanar model, the best fit was obtained with the triangular spins having smaller moments, $\langle M \rangle^{\mathrm{II}}_{\mathrm{tri}} = 1.3 \mu_{\mathrm{B}}$, than the kagome spins, $\langle M \rangle^{\mathrm{II}}_{\mathrm{kag}} = 2.0 \mu_{\mathrm{B}}$ (green on-line line in fig. 1(d)), which is more or less what a recent powder diffraction study has proposed [17]. In any case, our unpolarized neutron scattering results clearly show for the first time that the two phase transitions in GeNi$_2$O$_4$ are due to changes in the triangular layers, and it makes sense that these are harder to order since their interactions are more frustrated. Our finding also explains the origin of the two distinct types of magnetic environment found in a recent muon-spin relaxation study [18].

Figure 1(b) shows the temperature dependence of the spin-flip (SF) and non-spin-flip (NSF) intensities of the reflection. The measured ratio of SF to NSF intensities is $I_{\exp}(\mathrm{SF})/I_{\exp}(\mathrm{NSF}) = 8.7(8)$ after the correction for the imperfect polarization efficiency, and it stays almost constant. The measured ratio can be best reproduced when we assume that all spins lie in the (111) plane, $I_{\mathrm{cal}}(\mathrm{SF})/I_{\mathrm{cal}}(\mathrm{NSF}) = 8.27$, and the agreement rapidly worsens when the spins are allowed to have an out-of-plane component. So we conclude that in phase II both kagome and triangular layer spins lie in the (111) plane with an unknown angle between them.

Can we interpret the ordering pattern in terms of exchange interactions? Since Ni^{2+} has e_g^2 electronic configuration, the dominant interactions are due to super-exchange between the e_g^2 electrons and surrounding $2p$ electrons of O^{2-}. It is well known as the Goodenough-Kanomori rules that such superexchange interactions are sensitive to the bond angle, θ. The interactions are very weak if $\theta \sim 90°$ while they are antiferromagnetic if $\theta > 90°$ with the strength that increases with increasing θ up to 180°. We considered the first five of these that involve one to two Ni-O-Ni or Ni-O-Ge superexchange steps (see fig. 2(a) and table 1). The Goodenough-Kanomori rules for these exchange paths imply that J_1, J_2, and J_3' should be weak, whereas J_3 and J_4 are comparably strong and antiferromagnetic ($=$ positive in our convention). This contrasts with ACr$_2$O$_4$ (A $=$ Zn, Cd, Hg) where Cr^{3+} ions have t_{2g}^3 configuration and the nearest-neighbor interactions due to direct overlap of neighboring t_{2g} orbitals are dominant.

Table 1: List of the n-th nearest-neighbor interactions in a spinel, AB_2O_4, up to $n = 4$ and their possible *super*exchange paths via anions (O) and A- or B-site transition metal ions. J, d, θ, n_B, and Z represent the coupling constant, the bond distance in a unit of $a/4$, the bond angle, the number of the exchange path, and the number of bonds, respectively. The symbol (I) stands for couplings being in $\langle 111 \rangle$ planes, (K) and (T) for those with neighboring kagome and triangular layers, respectively. Z_K and Z_T are the number of bonds per a kagome and per a triangular spin, respectively. According to Goodenough-Kanamori rules, when B ions have e_g electrons, the superexchange BOB is sensitive to the bond angle: it can be ferromagnetic (for $\theta \leqslant 96°$) or antiferromagnetic (for $\theta \geqslant 96°$).

J	d	Path	θ	n_B	Z_K	Z_T
J_1	$\sqrt{2}$	BOB	$90°$	2	4 (I), 2 (T)	6 (K)
J_2	$\sqrt{6}$	$BOAOB$	$125°, 125°$	1	4 (I), 4 (K), 4 (T)	12 (K)
		$BOBOB$	$90°, 90°$	4		
J_3	$\sqrt{8}$	$BOAOB$	$125°, 125°$	2	2 (I), 4 (K)	6 (I)
J_3'	$\sqrt{8}$	$BOBOB$	$90°, 90°$	4	4 (I), 2 (K)	6 (T)
J_4	$\sqrt{10}$	$BOAOB$	$125°, 125°$	1	8 (K), 4 (T)	12 (K)

It is to be noted that, as there is no structural distortion, the spin layers form through a spontaneous symmetry breaking (in which one of the four $\{\frac{1}{2}, \frac{1}{2}, \frac{1}{2}\}$ ordering vectors is arbitrarily chosen). In fact, the "triangular" sites just consist of one of the four fcc sublattices of the pyrochlore structure, while the "kagome" sites are the union of the other three fcc sublattices. We considered candidate states with collinear spins in which each sublattice might independently have ordering vector $\boldsymbol{Q} = \{1, 0, 0\}$, $\boldsymbol{Q} = \{1, 1, 0\}$, or $\boldsymbol{Q} = \{\frac{1}{2}, \frac{1}{2}, \frac{1}{2}\}$ (either aligned or not with that sublattice's unique $\{111\}$ axis), focusing on spin arrangements competitive with the observed $\boldsymbol{Q} = (\frac{1}{2}, \frac{1}{2}, \frac{1}{2})$ pattern, when J_3, and J_4 are assumed strong and antiferromagnetic. In the observed structure, the triangular and the kagome layers have different mean-field energies per spin:

$$E_{\text{kag}} = 2J_1 - J_3 + J_3' - 4J_4, \tag{1a}$$

$$E_{\text{tri}} = 3J_3 - 3J_3', \tag{1b}$$

obtained using the counts in table 1. This gives a net energy/spin $E_{\text{tot}} = \frac{3}{4}E_{\text{kag}} + \frac{1}{4}E_{\text{tri}} = \frac{3}{2}J_1 - 3J_4$. By comparison, structures built from $\boldsymbol{Q} = (100)$ or (110) would give $E_{\text{tot}}^* = -J_3 - J_3' + 3J_6 \pm |J_1 - 2J_2 + 2J_4|$. Thus necessary condition to stabilize the actual structure is $E_{\text{tot}} < E_{\text{tot}}^*$, implying

$$J_4 > \frac{5}{2}J_1 - 2J_2 + J_3 + J_3', \tag{2}$$

which is plausible for $GeNi_2O_4$. Note that when J_4 dominates, the observed phase-I pattern of kagome layers with disordered triangular layers is the most stable mode in a mean-field approach.

As to the ordering temperatures, mean-field theory predicts $k_B T_{N1} = \frac{2}{3}|E_{\text{kag}}|$ and $k_B T_{N2} = \frac{2}{3}|E_{\text{tri}}|$, so $T_{N2} \lesssim T_{c1}$ implies (using (1a) and (1b)) that $J_4 - J_{1/2} \gtrsim J_3' - J_3$, which is consistent with the Goodenough-Kanamori rules. However, those rules would suggest $E_{\text{tri}} \approx 3J_3 > 0$, so it is surprising that T_{N2} is close to T_{N1}. Indeed, to ensure that the triangular spins order with the same $\boldsymbol{Q} = (\frac{1}{2}, \frac{1}{2}, \frac{1}{2})$ as the others (rather than the competing wave vectors), we must have $J_3' > J_3$; J_3' may be antiferromagnetic and J_3 ferromagnetic.

A remaining question is, what causes *both* kagome and triangular spins to point within the plane of the layers? It cannot be the uniaxial anisotropy of each spin (with respect to its local threefold axis): when averaged over the three sublattices forming the kagome spins, this must have a sign *opposite* to the anisotropy of the triangular spins (since the anisotropy of all four sublattices averages to zero). Nor can it be interlayer Dzyalohinski-Moriya (DM) couplings: these cancel by symmetry since the spins are ferromagnetic in each layer. The simplest explanation of the observed spin orientations is thus dipolar anisotropy. (Anisotropic exchange couplings will also generate an effective anisotropy for either kind of spin layer, the sign of which depends on the details of the anisotropy and the competition among the exchange interactions.)

In conclusion, our analysis suggests that in $GeNi_2O_4$, J_4 is the key interaction driving the first phase transition at T_{N1}. However, two discrepancies suggest our exchange-interaction model is incomplete in describing the triangular-layer behavior: i) the exchange theory would actually predict helimagnetic order with $\boldsymbol{Q} = (\frac{1}{2} + \delta, \frac{1}{2} + \delta, \frac{1}{2} + \delta)$ (with $|\delta| \gtrsim 0.01$), in analogy to a J_1-J_2 chain with $J_2 \gg |J_1|$, contrary to the observation in $GeNi_2O_4$ (as well as related compounds). ii) The exchange theory indicates FM J_3 and AFM J_3', which is unlikely according to the Goodenough-Kanamori rules. A complete understanding may require models with anisotropic interactions or disorder, as well as spin-wave experiments to better constrain the $\{J_i\}$.

$* * *$

REFERENCES

[1] Ramirez A. P., *Handbook of Magnetic Materials*, edited by Buschow K. J. H., Vol. **13** (Elsevier, Amsterdam) 2001.

[2] Bramwell S. T. and Gingras M. J. P., *Science*, **294** (2001) 1495.

[3] Moessner R. and Chalker J., *Phys. Rev. Lett.*, **80** (1998) 2929; *Phys. Rev. B*, **58** (1998) 12049.

[4] Canals B. and Lacroix C., *Phys. Rev. Lett.*, **80** (1998) 2933; *Phys. Rev. B*, **61** (2000) 1149.

[5] Lee S.-H. *et al.*, *Nature*, **418** (2002) 856.

[6] Hizi U. and Henley C. L., *J. Phys.: Condens. Matter*, **19** (2007) 145268.

[7] Lee S.-H. *et al.*, *Phys. Rev. Lett.*, **84** (2000) 3718.

[8] Chung J.-H. *et al.*, *Phys. Rev. Lett.*, **95** (2005) 247204.

[9] Matsuda M. *et al.*, *Nat. Phys.*, **3** (2007) 397.

[10] Tsunetsugu H. and Motome Y., *Phys. Rev. B*, **68** (2003) 060405(R).

[11] Lee S.-H. *et al.*, *Phys. Rev. Lett.*, **93** (2004) 156407.

[12] Zhang Z. *et al.*, *Phys. Rev. B*, **74** (2006) 014108.

[13] Crawford M. K. *et al.*, *Phys. Rev. B*, **68** (2003) 220408(R).

[14] Bertaut E. F. *et al.*, *J. Phys. (Paris)*, **25** (1964) 516.

[15] Izyumov Yu. A., Naish V. E. and Ozerov R. P., *Neutron Diffraction of Magnetic Materials* (Plenum Publishing Corporation, New York) 1991.

[16] Champion J. D. M. *et al.*, *Phys. Rev. B*, **64** (2001) 140407(R).

[17] Diaz S. *et al.*, *Phys. Rev. B*, **74** (2006) 092404.

[18] Lancaster T. *et al.*, *Phys. Rev. B*, **73** (2006) 184436.